Submitted to Ferroelectrics, 9/15/2002

Ferroelectric Phase Transitions in Nano-scale Chemically Ordered $PbSc_{0.5}Nb_{0.5}O_3$ using a First-principles Model Hamiltonian

Umesh V. Waghmare[†]
Theoretical Sciences Unit, JNCASR, Jakkur, Bangalore, 560 064 INDIA
Eric J. Cockayne and Benjamin P. Burton
Ceramics Division, NIST, Stop 8520, Gaithersburg, MD 20899, USA

Effects of chemical order, disorder, short range order, and anti-phase boundaries on phase transitions and dielectric properties of $PbSc_{1/2}Nb_{1/2}O_3$ are studied through molecular dynamics simulations of a FP model. Simulations of large systems are required to capture these effects, and we present an efficient reciprocal space method, based on fast Fourier transforms, for calculating long-range interactions and inhomogeneous strain. Calculations for random or partially disordered systems yield significant increases in T=0K dielectric response, and broadening of the ferroelectric phase transition. Coupling between random fields caused by chemical disorder and the inhomogeneous strain (acoustic modes) affects the dynamics of soft modes in chemically nano-structured configurations.

PACS numbers:

I. INTRODUCTION

Relaxor ferroelectrics (RFE) [1, 2] are technologically important materials with extraordinary dielectric properties. The temperature (T) and frequency dependence of the dielectric constant, $\epsilon(T,\omega)$, exhibits Vogel-Fulcher behavior[3] and are the characteristics of RFE, that distinguish them from conventional ferroelectrics (FE)[4]. As a function of T, $\epsilon(T,\omega)$ in a RFE exhibits a broad peak that is associated with a diffuse phase transition; and there is nontrivial dispersion over more than 10 decades of frequencies, clearly indicating processes that occur at several time-scales.

Most RFE exhibit these properties in both single-crystal and polycrystalline ceramic forms, and most RFE are ABO_3 perovskite based solid solutions of the form $A(B,B')O_3$ or $[AA']BO_3$ with heterovalent cations B and B' (e.g. Sc^{3+}, Nb^{5+}), or A and A' (e.g. Na^{1+}, Bi^{3+}). The degree of A- or B-site cation ordering is known to be strongly coupled to RFE properties[2]. Chemical order parameter (η) fluctuations on a scale of 10 nm[1] define nano-scale[5] heterogeneities with intense random fields (RF)[6]. Coupling between these RF and FE degrees of freedom (DOF) are thought to cause the formation of nano polar regions (PNR) with collective dipole moments.

$PbSc_{\frac{1}{2}}Nb_{\frac{1}{2}}O_3$ (PSN)[18, 12] and $PbSc_{\frac{1}{2}}Ta_{\frac{1}{2}}O_3$ (PST)[5] are two RFE, in which samples with varying degrees of B-site cation order[7] have been synthesized. They are therefore interesting systems in which to study the effects of cation order-disorder on RFE properties. When fully ordered, by ong annealing, PST exhibits a normal first-order FE phase transition, but results for well ordered PSN have not been reported [18]. The FE transition becomes diffuse when chemical disorder is introduced and the presence of polar nano regions (PNR)[5] in RFE is inferred from X-ray diffraction measurements.

Phenomenological models of RFE provide a basis for fitting and interpreting experimental data, e.g. the spherical random bond random field (SRBRF) model, is based on the concept of mutually interacting PNR in the presence of RF that are associated with chemical disorder or vacancies. This explains many characteristics of RFE that are related to their glassy properties in the low-temperature phase[13]. The dynamics of RFE domains[14] and a model relaxation time spectrum[15] is invoked to describe the Vogel-Fulcher behavior of $\epsilon(T,\omega)$ in a limited temperature range. Validations of phenomenological model characteristics, and a unified description of a wide range of RFE properties requires microscopic models.

Neutron scattering and diffraction experiments[17–19] revealed interesting data on soft and acoustic mode anomalies, and structure. Other experiments[20] based on x-ray diffuse scattering indicate antiferroelectric (AFE) type local ordering in PSN, raising additional questions. Atomistic simulations can resolve the issues related to vibrational excitations and their couplings with chemical heterogeneities at different length-scales.

Microscopic lattice dynamical models for PSN were constructed from the results of first-principles (FP) calculations[23, 22] for PSN and were used in Monte Carlo simulations to study the statics of phase transition behavior. The size of systems ($\tilde{1}$2x12x12 unit cells) used in this simulations is too small to include realistic chemical inhomogeneities. Simulations for larger systems have been limited by the long-range dipolar interactions whose

computation scales as $O(N^2)$. We present an FFT-based method in mixed space which efficiently treats both dipolar interactions and inhomogeneous strains. This approach is easily applied in energy minimizations and molecular dynamics (MD) simulations, and it scales as $O(NlogN)$. Preliminary results are presented for systems with chemical order that is: 1) Fully ordered, $\eta = 1$; 2) Random, $\eta = 0$; 3) nanoscale mixtures of ordered and disordered regions. Zero-T nonlinear hysteretic properties [22], and Finite-T transitions are calculated.

II. GENERAL FORM OF THE MODEL AND THE MIXED SPACE METHOD

Here we present methods for $T = 0$K energy minimization, and $T \neq 0$ MD, that scale as $O(NlogN)$, and therefore, allow large-scale (40x40x40 unit cell) simulations. The aim is to simultaneously update all DOF, based on known forces and energies. The FP model Hamiltonian, H, was derived via the method of Lattice Wannier Functions (LWF) [24]. H is a symmetry-invariant (of space group $Pm\bar{3}m$) Taylor expansion in terms of strain and LWFs which span a subspace of structural excitations with respect to atomic displacements and uniform deformations that are lowest in energy. To simplify, one identifies bands of unstable phonons (*lattice instabilities*) and maps atomic displacements into the corresponding localized LWF. DOF in the model, LWFS, are 2 or 3-d classical vectors (pseudospins), which map precisely onto atomic displacements via the LWF[24, 25].

In the PSN model[22], there are two sets of classical vectors used as DOF:$\{ \vec{\xi}_i \}$ and $\{ \vec{\eta}_i \}$; i indexes the i'th unit cell. The $\vec{\xi}_i$'s are polar DOF which carry dipole moments given by the mode effective charge, and span the unstable band of optical phonons. $\vec{\eta}_i$'s are nonpolar and span acoustic phonon bands. An additional six DOF correspond to symmetric homogeneous strain $e_{\alpha\beta}$. Chemical order is defined by Ising pseudospin DOF, σ_i, such that $\sigma_i = -1$ for Sc, and $\sigma_i = +1$ for Nb. H is essentially a Taylor series in $\vec{\xi}_i$, $\vec{\eta}_i$ and $e_{\alpha\beta}$ in which the coefficients are determined from FP calculations. Dependence of these coefficients on the σ_i encodes the RF-effects of chemical order-disorder.

Note that the $\vec{\eta}_i$'s describe inhomogeneous deformations of the crystal; in the long wave-length limit they essentially yield the elastic energy. Periodic boundary conditions exclude the homogeneous deformation from the subspace spanned by $\vec{\eta}_i$'s, so it is included through six explicit symmetric strain tensor components $e_{\alpha\beta}$.

The model hamiltonian is:

$$H = \sum_i P_8(\vec{\xi}_i) + \sum_{ij,\alpha\beta} J^{\alpha\beta}_{i-j}\xi_{i,\alpha}\xi_{j,\beta} + \sum_{ij} A^{\alpha\beta}_{i-j}\eta_{i,\alpha}\eta_{j,\beta} + \sum_{ij} G_{i-j,\alpha\beta\gamma}\eta_{i,\alpha}\xi_{j,\beta}\xi_{j,\gamma} + \sum_{\alpha\beta\gamma\delta} C_{\alpha\beta\gamma\delta}e_{\alpha\beta}e_{\gamma\delta} + \sum_{\alpha\beta} g_{\alpha\beta\gamma\delta}e_{\alpha\beta}\xi_{j,\gamma}\xi_{j,\delta} \sum_{ij} D_{ij\alpha}S_i\xi_{i,\alpha} \quad (1)$$

where: P_8 is a polynomial of order 8; J are quadratic interaction parameters for the polar DOF which include long-range polar and short-range interactions; A are the harmonic force constants for the acoustic DOF, G gives the third order coupling between ξ and η; C are the elastic constants; $i-j$ indicates that the interaction parameter depends on the distance between the teo sites; g is the coupling between homogeneous strain and ξ; and D is the local field exerted on ξ by the chemical environment defined by σ_i. Note that the effect of chemical environment on $\vec{\xi}$ is over simplified in the above form, but what follows applies to a more general models as well.

In conventional simulations this model is computationally demanding because: (1) the long-range dipolar interactions between $\vec{\xi}_i$'s necessitate the computation of interactions between each spin and all others; (2) elastic and interactions of the $\vec{\eta}_i$s extend up to third neighbors, and are often slow DOF. In small systems, these DOF have no effects on the statics of FE transitions, but we expect them to be important for dynamics, particularly in chemically inhomogeneous RFE. Other terms in the model are local in real space ("on-site") and can be treated quite efficiently. Long-range interactions are treated with efficient FFT algorithms. DOF in real and reciprocal space are related by:

$$\xi_\alpha(q) = \frac{1}{N}\sum_i e^{(-i\vec{q}\cdot\vec{r}_i)}\xi_{i,\alpha}, \quad (2)$$

where $\vec{r}_i$ is the position vector of the ith point on the lattice and q also belongs to a lattice in reciprocal space:

$$\vec{q} = (i,j,k)\frac{2\pi}{a}, \quad (3)$$

a being the lattice constant, and i, j and k are integers in the interval $(-\frac{L}{2}, \frac{L}{2}-1)$, L being the linear size of the finite system being studied in a simulation ($N = L^3$). Similarly,

$$\xi_{i\alpha} = \sum_{\vec{q}} e^{(i\vec{q}\cdot\vec{r}_i)}\xi_i(\vec{q}) \quad (4)$$

A Long-range Intersite Interactions

To treat long-range interactions efficiently we exploit the translationally invariant part of the intersite interactions (those which depend on the distance vector $\vec{r}_i - \vec{r}_j$) as local in reciprocal space:

$$E_{int} = \sum_q \xi_\alpha(-q) J_{\alpha\beta}(q) \xi_\beta(q), \tag{5}$$

where $J_{\alpha\beta}(q)$ is the Fourier transform of $J^{\alpha\beta}_{i-j}$. Thus, the force on $\xi_\alpha(q)$ arising from these interactions is simply

$$F_\alpha(q) = -\sum_\beta J_{\alpha\beta}(q) \xi_\beta(q). \tag{6}$$

This is inverse Fourier transformed to obtain the force on $\xi_{i\alpha}$. We include both long-range dipolar and short-range intersite interactions in the coupling J and obtain its Fourier transform once at the beginning of the simulation. The effects of chemical order generally affect intersite interactions, and that must be treated in real space. However, these effects are expected to be short-range, and the reciprocal space treatment of dipolar interactions space is still useful. A flow-chart is given in Fig. 1(a).

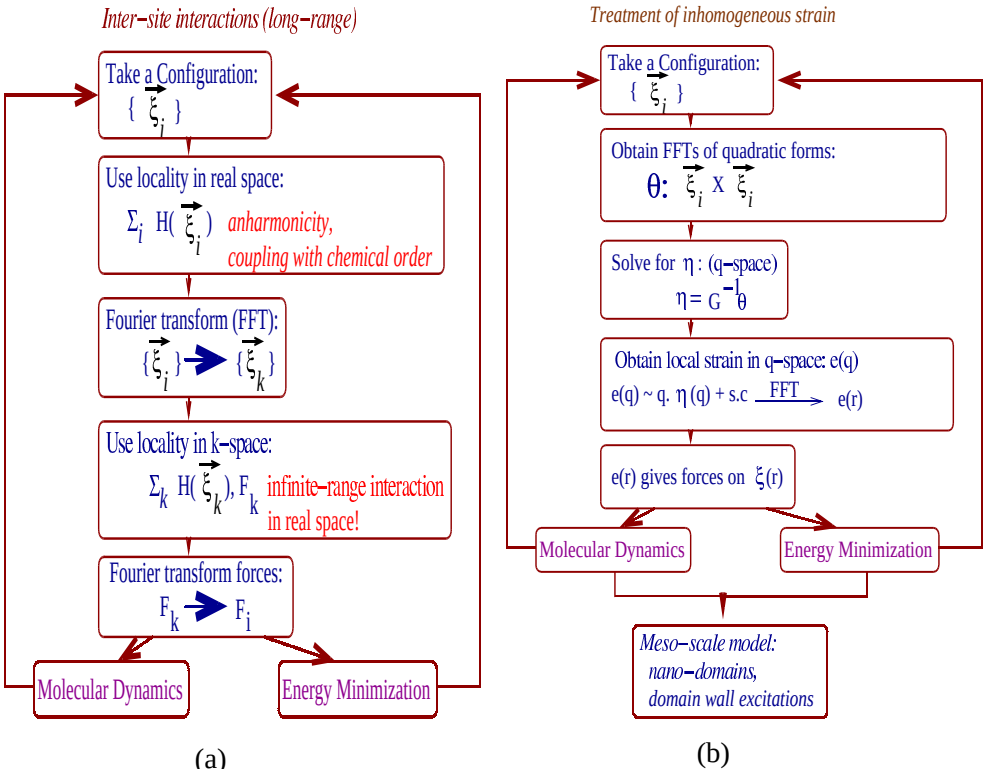

FIG. 1: Flow-charts for simulations based on FFTs: (a) intersite interactions of model FE; (b) inhomogeneous strain.

B Inhomogeneous Strain

The parameters A and C (G and g) are related in the long wave-length limit:

$$A_{\alpha\beta}(q) = \sum_{\gamma\delta} q_\gamma q_\delta (C_{\alpha\gamma\delta\beta} + C_{\gamma\alpha\delta\beta} + C_{\alpha\gamma\beta\delta} + C_{\gamma\alpha\beta\delta}) \tag{7}$$

and

$$G_{\alpha\gamma\delta}(q) = \sum_{\beta} iq_{\beta}(g_{\alpha\beta,\gamma\delta} + g_{\beta\alpha,\gamma\delta}), \tag{8}$$

where $\vec{q}$ is a wave vector and $A(q)$ and $G(q)$ are Fourier transforms of the A_{i-j} and G_{i-j} respectively. It is clear that $A(q)$ and $G(q)$ vanish as q^2 and q in the $q \to 0$ limit. This is essentially a result of acoustic sum rule; that uniform displacement of a crystal does not cost any energy. The power of q in the limiting behavior of A and G is determined by the fact that these parameters give energetics of inhomogeneous strain $e_{\alpha\beta}(r)$ at second and first order respectively and the reciprocal space strain is given by:

$$e_{\alpha\beta}(q) = \frac{1}{2}(q_{\alpha}\eta_{\beta}(q) + q_{\beta}\eta_{\alpha}(q)) \tag{9}$$

where $\eta_{\alpha}(q)$ is the Fourier transform of $\eta_{\alpha}(r)$.
The $\eta-$dependent part of the model is easily written in reciprocal space:

$$E_{inh} = \sum_{\alpha\beta,q} A_{\alpha\beta}(q)\eta_{\alpha}(-q)\eta_{\beta}(q) + \sum_{q,\alpha\beta\gamma} G_{\alpha\beta\gamma}(q)\eta_{\alpha}(-q)\Theta_{\beta\gamma}(q), \tag{10}$$

where $\Theta_{\beta\gamma}(q)$ is the Fourier transform of $\xi_{\beta}(r)\xi_{\gamma}(r)$. In reciprocal space, $\eta_{\alpha}(q)$'s form non-interacting DOF coupled to ξ's locally at each q. Also, the energy terms in $\eta(q)$ are only quadratic and linear, they can be integrated out exactly for a given configuration of $\vec{\xi_i}$'s through a simple minimization with respect to three η components:

$$\eta_{\alpha}(q) = -\sum_{\beta} A^{(-1)}_{\alpha\beta}(q) \sum_{\beta\gamma} G_{\alpha\beta\gamma}\Theta_{beta,\gamma}(q). \tag{11}$$

In practice, we construct the q-dependent inverse elastic matrix at the beginning of a simulation. Instantaneous configuration of $\eta_{\alpha}(q)$'s is obtained from Eqn 11, which subsequently gives an additional force on the $\vec{\xi_i}$ DOF. Thus, we completely eliminate numerical minimization or dynamics of $\eta-$ DOF. We do have access to values of local strain throughout the simulation and hence its averages or optimal values. Practical implementation of this algorithm is illustrated in Figure 1.

III. DIFFERENT NANO-SCALE CHEMICALLY ORDERED CONFIGURATIONS

In PSN, a chemical order-disorder transition takes place at 1210^0 C[7] below which Sc^{3+} and Nb^{5+} order into a NaCl-type superstructure, and above which they are disordered . Depending on the heat treatment[8], PSN may form with various degrees of order, or as nanotextured (non equilibrium) mixtures of ordered and disordered phases. We consider configurations with different degrees of chemical, or ordered + disordered textures, and assume that these might be obtained by appropriate heat treatment or synthesis technique:

- (O) A fully ordered configuration with a NaCl-type substructure of Sc and Nb on the B-sites
- Random configuration (R)
- Ordered domains separated by anti-phase boundaries (APB). The $40 \times 40 \times 40$ unit cell is divided into 8 equal NaCl-type ordered domains (octants) that are separated by *wetted* APBs 6 unit cells wide. Inside the APBs 15 % of the sites are randomly occupied, and the volume fraction of the system that is disordered is $\phi_{Dis} = 0.657$.
- Superlattice, $SL_{O:D}$, e.g. the configuration $SL_{8:12D}$ is a periodic array of ordered and disordered slabs that are 8 and 12 unit cells thick, respectively. Thus, $\phi_{Dis} = 0.50$. for $SL_{10:10D}$, $\phi_{Dis} = 0.60$ for $SL_{8:12D}$.
- Nano-domain (NO) this configuration is generated by placing 20 spherical domains of chemically ordered PSN, diameter $\sim$10 unit cells, that are randomly located in the $40 \times 40 \times 40$ system. To avoid domain overlaps, site occupations between ordered domains are random; $\phi_{Dis} = 0.60$.

Schematic pictures of these configurations are given in Fig 2.

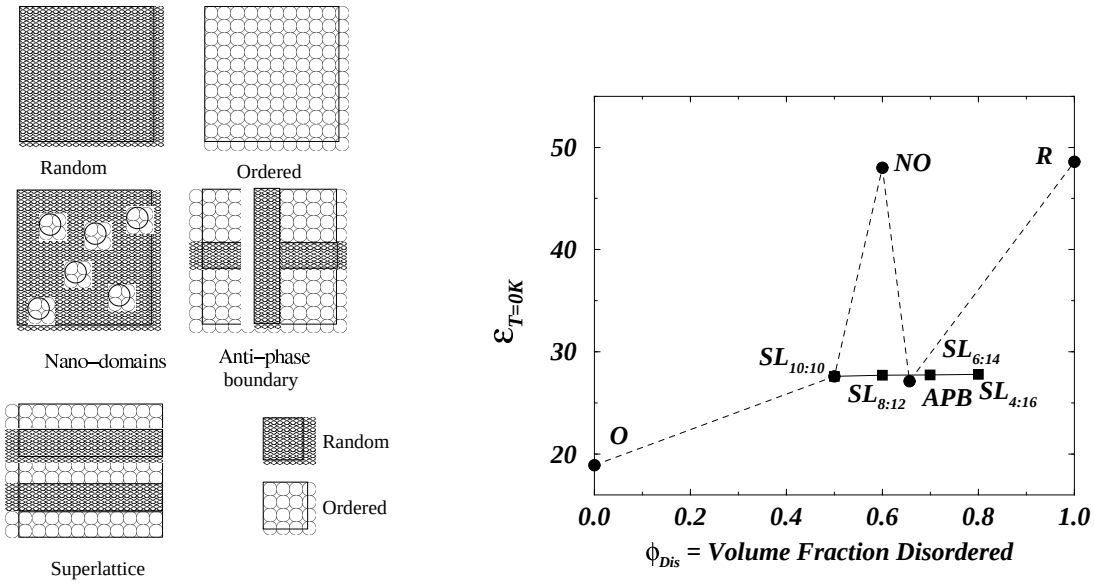

FIG. 2: (a) Schematic of various nano-scale chemically ordered configurations (Figure not to scale); (b) $T = 0$K dielectric response as a function of the disordered volume fraction for configurations (O=Ordered, $SL_{O:D}$=Superlattice, NO=Nano-domain, APB=Antiphase Boundary, R=Random).

IV. RESULTS AND DISCUSSION

$T = 0$K properties are simulated by energy minimization via a conjugate-gradient algorithm[26] to find the initial estimate of the minimum, and convergence is improved with a line-minimization steepest descent algorithm[26]. This is essential for configurations with some disorder for which energy minimization is slow; consistent with the glassy nature of RFE, inferred from experiments and phenomenological models[13]. Figure 2(b), exhibits a generally positive but **not monotonic** trend for $\epsilon_{T=0K}$ as a function of ϕ_{Dis}. Clearly, the RF-microstructure, which is dictated by local fluctuations of chemical order, has significant nonlinear effects on $\epsilon_{T=0K}$.

Figures 3 compare finite-T simulations with, and without, inhomogeneous strain, for the ordered and nano-domain configurations. Clearly, the $\epsilon(T)$ curve for the nano-domain configuration (d) is broadened significantly relative to the ordered configuration, **when inhomogeneous strain is included.** Also, the Edwards-Andersen order parameter, $q_{EA}(T)$, appears to exhibit significant deviation from zero at $T > T_{FE}$, the FE phase transition in these simulations; this result is indicates significant structural disorder for a wide range of temperature above T_{FE}. As in previous simulations [22, 23] these predict $T_{FE}(OrderedPhase) > T_{FE}(PartiallyOrdered) > T_{FE}(Disordered)$ consistent with experiments for PST [11], but apparently contradicting results for PSN [10, 12, 8, 18]. Note however, that sample characterization results presented in Perrin et al. [18] clearly indicate a **nonequilibrium** two-phase assemblage in their most ordered sample. Genuinly single-phase samples with high degrees of chemical order might exhibit the same transition sequence as PST and the simulations. If, however, $T_{FE}(OrderedPhase) < T_{FE}(PartiallyOrdered) < T_{FE}(Disordered)$ is the correct trend for PSN, then it seems likely that a more complex effective Hamiltonian will be required to correctly simulate PSN; specifically, a model Hamiltonian that explicitly includes both Nb- and Pb-displacements.

ACKNOWLEDGMENTS

UVW acknowledges useful discussions with Sereguei Prosandeev and M H Cohen.

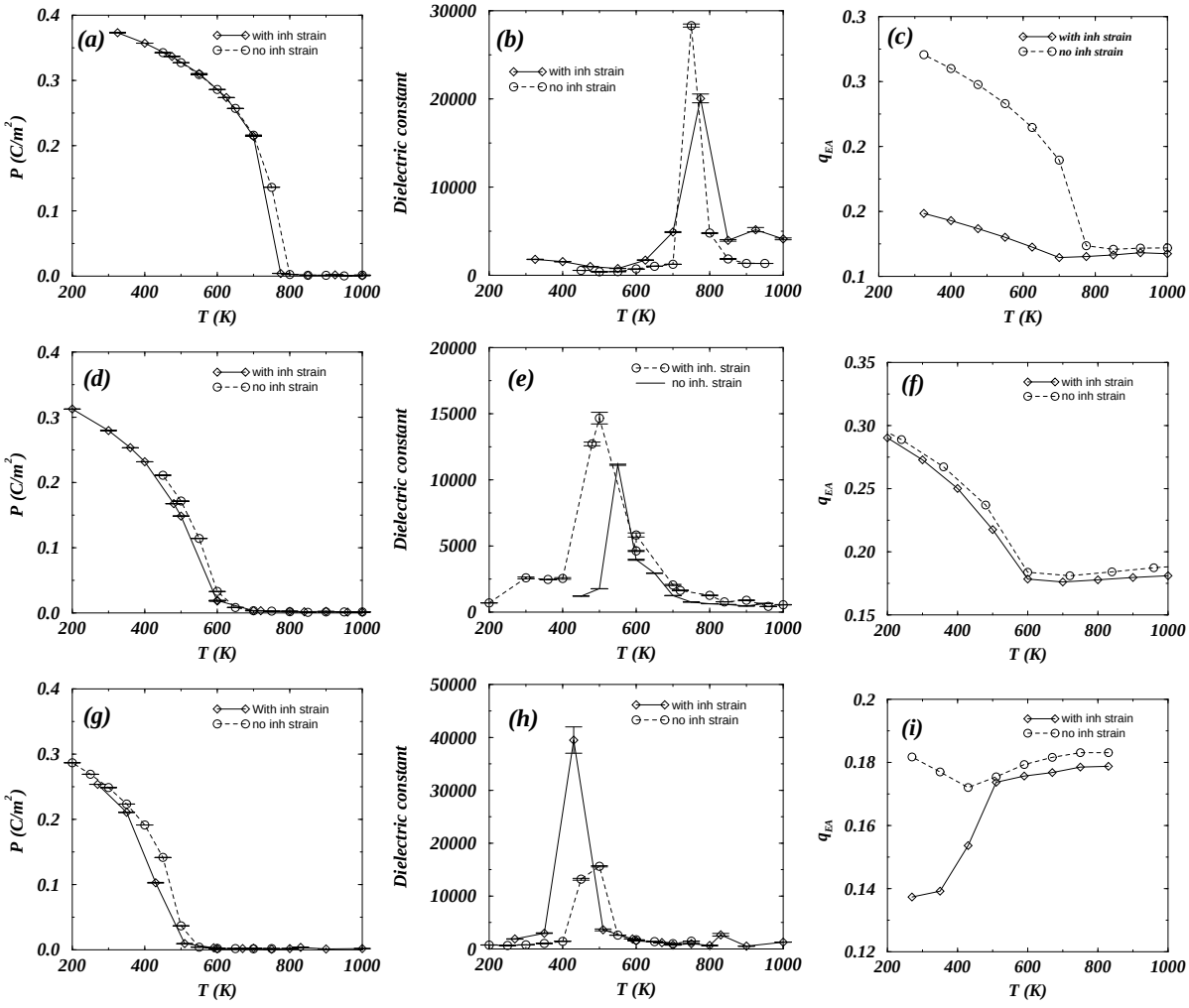

FIG. 3: Finite temperature results for: (a-c) Ordered; (d-f) Nano-domain; (g-i) Random convigurations. Simulated properties are: Polarization (a,d,g); dielectric constant (b,e,h); Edwards-Anderson order parameter (c,f,i).

REFERENCES

† Electronic address: e-mail:waghmare@jncasr.ac.in

[1] G. A. Smolensky, A. I. Agranovskaya, Sov. Phys. Sol. State **1**, 1429 (1959).
[2] L. E. Cross, Ferroelectrics **76**, 241 (1987).
[3] D. Viehland, S. J. Jang, L. E. Cross and M. Wuttig, J. Appl. Phys. **68**, 2916 (1990).
[4] M. E. Lines and A. M. Glass, *Principles and Applications of Ferroelectrics and Related Materials*, Clarendon Press, Oxford (1979).
[5] N. Setter and L. E. Cross, J. Appl. Phys. **51**, 4356 (1980).
[6] V. Westphal, W. Kleemann and M. D. Glinchuk, Phys. Rev. Lett. **68**, 847 (1992).
[7] C. G. F. Stenger and A. J. Burggraaf, Phys. Stat. Sol. **a 61**, 274 (1980).
[8] C. Perrin, N. Menguy, O. Bidault, C.Y. Zahra, A-M Zahra, C. Caranoni, B. Hilczer and A. Stepanov J. of Phys. Cond Matt **13**, 10231 (2001).
[9] M. P. Harmer, J. Chen, P. Peng, H. M. Chan and D. M. Smyth, Ferroelectrics **97**, 263 (1989).
[10] F. Chu, I. M. Reaney and N. Setter, J. Appl. Phys. **77**, 1671 (1995).
[11] F. Chu, I. M. Reaney and N. Setter, J. Am. Ceram. Soc. **78**, 1947 (1995).
[12] C. Malibert, B. Dkhil, J. M. Kiat, D. Durand, J. F. Berar and A. Spasojevic-de Bire, J. of Phys. Cond Matt **9**, 7485 (1997).
[13] R. Blinc, J. Dolinsek, A. Gregorovic, B. Zalar, C. Filipie, Z. Kutjnak, A. Levstik and R. Pirc, Phys. Rev. Lett. **83**, 424 (1999).
[14] A. E. Glazounov, A. K. Tagantsev and A. J. Bell, Phys Rev **B53**, 11281 (1996).
[15] A. K. Tagantsev, Phys. Rev. Lett. **72**, 1100 (1994).
[16] Fan Chu, G. R. Fox and N. Setter, J. Am. Ceram. Soc. **81**, 1577 (1998).
[17] P. M. Gehring, S.-E. Park and G. Shirane, Phys. Rev. Lett. **84**, 5216 (2000).
[18] C. Perrin, N. Menguy, E. Suard, Ch Muller, C. Caranoni and A. Stepanov, J. of Phys. Cond Matt **12**, 7523 (2000).
[19] T. Y. Koo, P. M. Gehring, G. Shirane, V. Kiryukhin, S.-G. Lee and S.-W. Cheong, Phys Rev **B 65**, 144113, (2002).
[20] N. Takesue, Y. Fujii, M. Ichihara and H. Chen, Phys. Rev. Lett. **82**, 3709 (1999).
[21] N. Takesue, Y. Fujii, M. Ichihara, H. Chen, S. Takemori and J. Hatano, J. of Phys. Cond Matt **11**, 8301 (1999).
[22] E. Cockayne, B. P. Burton and L. Bellaiche, Fundamental Physics of Ferroelectrics 2001, Ed. H. Krakauer, AIP Conference Proceedings 2001.
[23] R. Hemphill, L. Bellaiche, A. Garcia and D. Vanderbilt, Appl. Phys. Lett. **77**, 3642 (2000).
[24] K. M. Rabe and U. V. Waghmare, Phys. Rev. B **52**, 13236 (1995).
[25] U. V. Waghmare and K. M. Rabe, Phys. Rev. B **55**, 6161 (1997).
[26] Numerical Recipes in Fortran.
[27] E. B. Tadmor, U. V. Waghmare, G. S. Smith and E. Kaxiras, Phys Rev B, in press.
[28] Jorge Iniguez and L. Bellaiche Phys. Rev. Lett. **87**, 095503 (2001).